sustainability

MDPI

Article

Rockfall Analysis for Preliminary Hazard Assessment of the Cliff of Taormina Saracen Castle (Sicily)

Simone Mineo [1], Giovanna Pappalardo [1,*], Michele Mangiameli [2], Santo Campolo [3] and Giuseppe Mussumeci [2]

[1] Department of Biological, Geological and Environmental Sciences, University of Catania, Corso Italia 57, 95129 Catania, Italy; smineo@unict.it
[2] Department of Civil Engineering and Architecture, University of Catania, Via Santa Sofia 54, 95125 Catania, Italy; michele.mangiameli@dica.unict.it (M.M.); g.mussumeci@dica.unict.it (G.M.)
[3] Regione Siciliana—Department of Cultural Heritage and Sicilian Identity, Viale Boccetta 38, 98100 Messina, Italy; santo.campolo@regione.sicilia.it
* Correspondence: pappalar@unict.it

Received: 15 December 2017; Accepted: 1 February 2018; Published: 6 February 2018

Abstract: A rockfall analysis at one of the most relevant cultural heritage sites of northeastern Sicily (Italy) is presented herein with the aim of assessing the hazard arising from the unstable conditions of the rock cliff of Taormina city, upon which the Saracen Castle is perched on its top. Several rockfalls affected this area in the latest years, representing a serious threat for the safety of inhabitants and tourists. Therefore, the qualitative Evolving Rockfall Hazard Assessment (ERHA) was applied for the hazard zonation, supported by rock mass surveys and Terrestrial Laser Scanner prospecting. Kinematic analysis revealed that the unstable rock failure patterns are represented by planar/wedge sliding and toppling, while simulation of potential rockfalls allowed studying the impact of future events in terms of trajectory and energy. This is higher at the foot of scarps and in steeper sectors, where the application of ERHA identified a critical zone close to the inhabited center, which is one of the main elements at risk, along with a pedestrian tourist path. Achieved results represent a starting point for the definition of risk management strategies and provide a scientific contribution to the study of hazard and risk arising from rockfall occurrence.

Keywords: Rockfall Hazard; cultural heritage; trajectory simulation; rock mass survey; LIDAR

1. Introduction

Slope instability is a serious condition affecting several rock cliffs over the world, upon which historical buildings are often perched (e.g., [1–3]). These are usually a part of ancient settlements, churches, and castles of cultural relevance, and represent key locations for rockfall risk management, due to their historical aspects and tourist attraction.

Rockfalls, caused by the detachment of a rock boulder from a slope, are fast and unpredictable landslide movements characterized by a rapid evolution in space; for this reason, they are among the most studied geomorphic processes worldwide, especially in mountainous areas (e.g., [4–6]). They can cause significant damage to structures and infrastructures, even when small rock volumes are involved, thus representing a relevant risk for goods and people (e.g., [7,8]). In particular, risk arising from rockfalls is defined as the probability of impact of an uncertain, sudden, and extreme hazardous event which can cause damages to one or more exposed elements (modified after [9,10]). Therefore, its assessment is an essential scientific procedure to achieve a zonation of the analyzed territory and to identify the main threatened elements, which are the targets exposed to the risk. Based on the economic and social impact of the expected event, these kinds of studies are crucial for risk management purposes, because they can be employed as a tool to locate and design proper mitigation

measures. To this purpose, several qualitative and quantitative approaches have been proposed in the scientific literature for the evaluation of hazard and risk arising from rockfalls (e.g., [8,11–21]). Some of these are empirical or semi-empirical methods, which take into account the probability of rock failures, while others involve a statistical analysis of the potential rockfall trajectories and the probability of bad-consequences after the event. For example, the Rockfall Hazard Rating System (RHRS) initially developed by Pierson et al. [22] is a rating approach to identify dangerous slopes that require urgent remedial works or further studies along transportation routes. Inspired by this method, Saroglou [15] developed a risk assessment procedure for natural slopes. On the other hand, probabilistic analyses are taken into account by the Rockfall risk Management method (Ro.Ma.), which is based on the construction of specific Event Trees to assess risk in peculiar conditions (e.g., [8,13,23]).

The choice of the approach to follow is not only a function of a predetermined aim, but it depends also on the availability of data and on the knowledge of the rockfall history of the study area. In particular, the case study presented herein is about a rockfall hazard zonation through the Evolving Rockfall Hazard Assessment procedure (ERHA) (e.g., [24,25]) at the promontory of the Saracen Castle of Taormina (NE Sicily, Italy). Perched on the top of a carbonate cliff, the castle is an example of cultural heritage dominating the city of Taormina, renowned from the tourist point of view. This location has suffered from the threat of rockfalls affecting cliff stability and, as a consequence, this threatens the safety of tourists traveling along the access trail to the castle. Its construction started in the Hellenic period on the top of Tauro Mount, about 400 m a.s.l. along the northeastern coast of Sicily (Figure 1). As a strategic military fort, it resisted several sieges and was defined as one of the most famous primitive castles in one of the noblest towns [26]. It can be reached through an 800 m long panoramic pedestrian stairway (PPS) from the city center. Due to the geological and geostructural setting of the area, along with its high seismicity, Taormina cliff is characterized by peculiar geomechanical features, which can be regarded as one of the main causes of slope instability. Although most of the events were not studied from the technical point of view, blocks usually detach from the highest portions of the cliff and move downstream, sometimes crossing PPS, which acts as a boulder rebound or an end point. In fact, several blocks were surveyed along its path and signs of the transit of past rockfalls are present (damage on the road pavement, broken railing). Moreover, most of falling blocks reach the foot of the cliff, where private buildings and the Road SP10 represent the main elements exposed to risk. In order to protect such elements, mitigation works were performed in the latest years, but they were limited only to specific portions of the cliff, while unstable blocks of considerable volume (about 0.15 m^3 referred to an average measure of the most relevant fallen blocks) still represent a serious threat to local people and tourists.

Figure 1. Geographical location of the study area and 3D model of Taormina territory (Google Earth): coordinates are referred to the Saracen Castle.

In this scenario, this paper presents a preliminary hazard assessment to highlight the most hazardous sectors of the cliff. The EHRA approach applied herein was developed for the Australian coal-mining environment and then employed for risk management in several studies worldwide (e.g., [24,25]). According to this procedure, outcrops of Taormina cliff underwent a geomechanical characterization through field surveys and geometry reconstruction by Terrestrial Laser Scanner (TLS). Rock mass surveys were carried out according to ISRM recommendations [27,28] by measuring dip-immersion, spacing, persistence, opening, and evaluating in-filling, roughness, uniaxial compressive strength (UCS), and hydraulic conditions of discontinuities. Kinematic analyses at the most critical spots allowed for the ascertaining of the predisposition of the rock to fail through peculiar kinematic patterns and rockfall trajectory simulations, which were modeled to estimate the intensity of potential events. Results were finally mapped to highlight the spatial distribution of an assessed hazard and its interaction with the main elements at risk.

2. The Saracen Castle of Taormina: A Mix of History and Geology

There is no precise information on the construction of the Taormina Saracen Castle, which dates back to the Hellenic period. It was employed as a military fortress by Arabian conquerors, thanks to its strategic location, which guaranteed a 360° view of the eastern coast of Sicily. The Arabian domain resisted until the kingdom of Earl Ruggero in 1079 A.D., while in 1240 A.D. the castle was counted among the goods belonging to King Frederik II. In 1297, during the Aragon dynasty, this fort was entrusted to the Taormina governor [29]. Nowadays, it is recognized as a cultural heritage, witness of the defensive architecture of XII and XIII centuries.

The carbonate cliff on which the castle is perched belongs to the Peloritani Mountain belt, a nappe pile orogen showing several S-SE verging tectonic slices characterized by a northward increasing metamorphic grade [30]. It is the southern part of the Calabria–Peloritani orogenic arc and consists of a Hercynian metamorphic basement, covered by Mesozoic–Cenozoic units (e.g., [30–32]). In the study area, the low-grade crystalline formations are overlapped by sedimentary deposits dated between Early Lias to Olocene (Figure 2). In particular, Lower Liassic greyish-white limestones and dolostones in carbonate platform facies represent the framework of the studied cliff (Figure 3a–c), which experienced several rockfall phenomena due to the intense degree of fracturing of the rock. Tectonics played a leading role over the geological times and it is responsible of the high seismic activity of the Peloritani region, characterized by the recurrence of several destructive historical earthquakes (e.g., [33]). In particular, tectonic activity in this area is testified by the presence of regional fault sets, striking W–E, NW–SE, and NNW–SSE, and some authors recognized uplift signs at several marine terraces occurring along the coast, with an average rate of 1.7 mm/year in the study area (e.g., [34,35] and references therein). According to Argnani et al. [36] and references therein, large and destructive earthquakes can be associated with fault activity along southeastern Sicily and southern Calabria faults, testifying to the link between tectonics and seismic activity in the study area. Moreover, tectonics is usually a predisposing factor to slope instability (e.g., [37] and references therein) due to the degree of fracturing of outcrops resulting from the mechanical response of the rock to field stresses.

With reference to Taormina cliff, about 130 m tall with respect to the city center, the occurrence of several rockfalls is testified by widespread fallen blocks, both at the foot of the cliff and along the slopes, and signs of past detachments on the cliff walls. Unfortunately, most of these events were never studied from a technical point of view, unless from few studies for local protection measures carried out in the past. Rockfalls usually originate from the top of the cliff, where several blocks stand in unstable conditions, and move downstream following the terrain morphology. Among the most recent events, the 2013 and 2015 rockfalls are two of the most hazardous: they originated by the detachment of about 0.10–0.15 m^3 boulders, which crossed the touristic PPS path, damaging its pavement and banister. Fortunately, no victims were reported, although blocks stopped along PPS representing a relevant risk for safety (Figure 3d–e). Such events were not isolated, and signs of past detachments can be identified by depletion areas on the rock face (Figure 3). Furthermore, the most worrying feature

for potential future detachments is the presence of several blocks in precarious equilibrium condition (Figure 3f) showing unfavorable kinematic setting (see next sections).

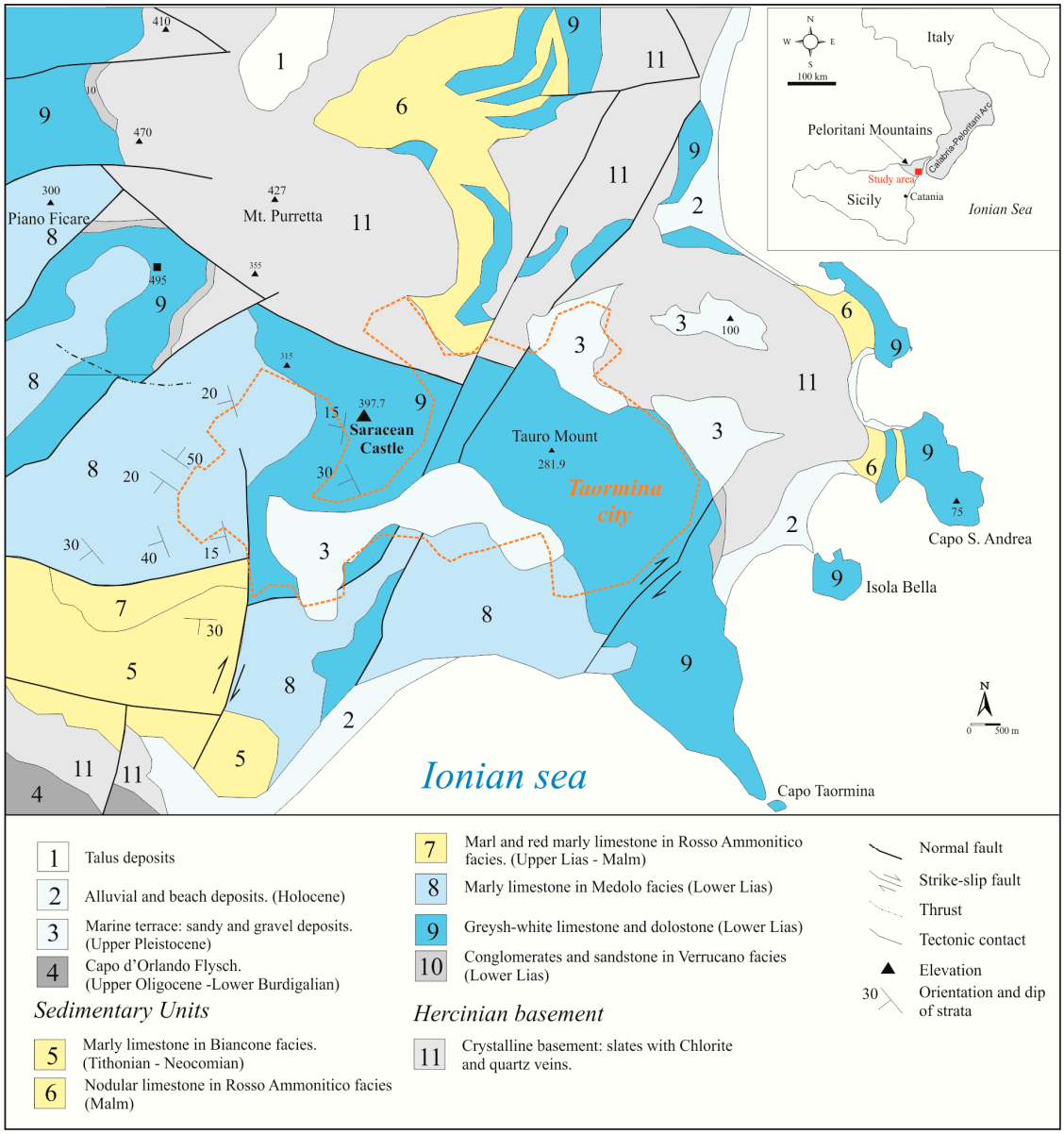

Figure 2. Schematic geological map of the study area (modified after [38]).

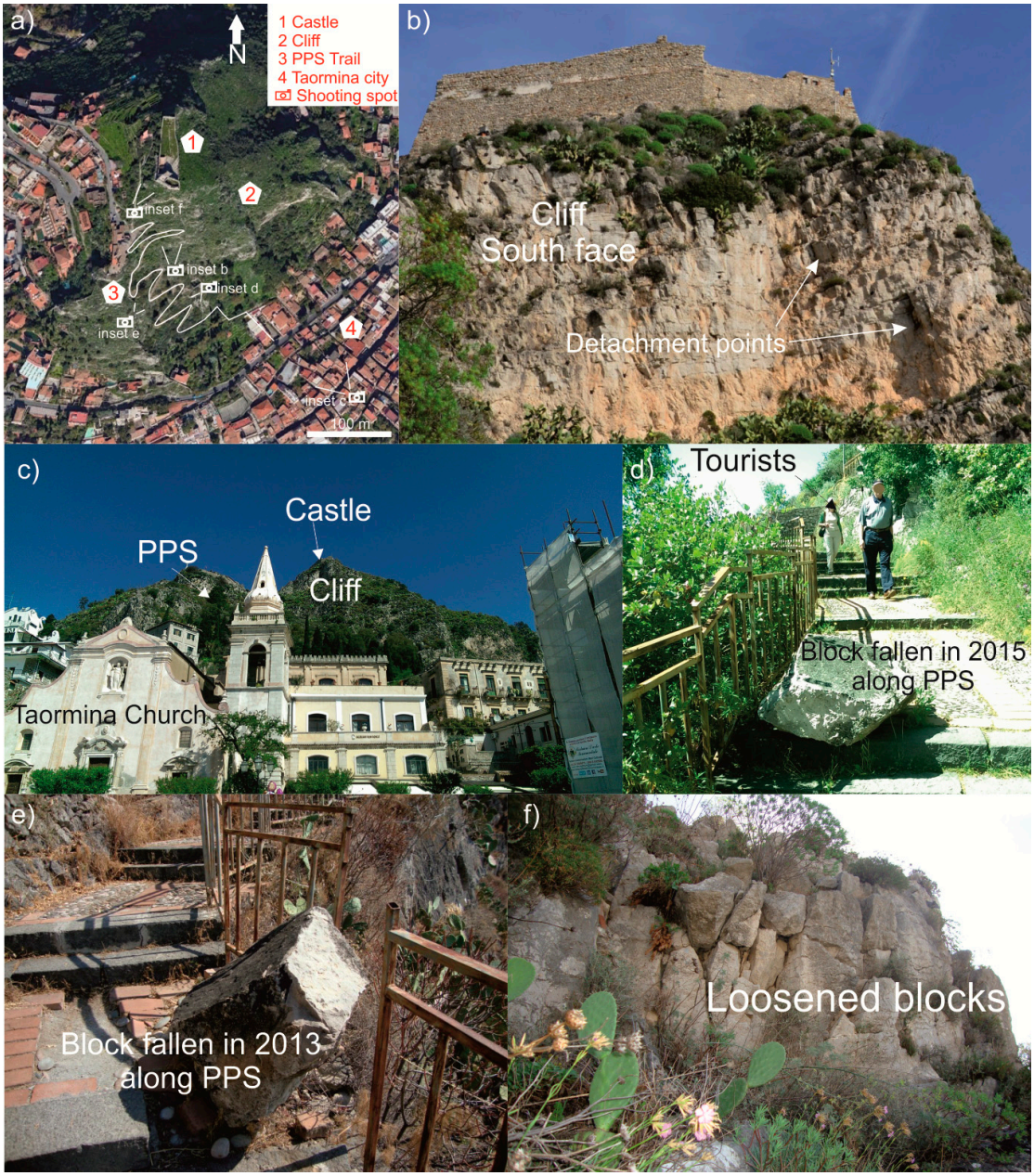

Figure 3. (**a**) Location of the main elements on a satellite image (PPS: panoramic pedestrian stairway); (**b**) a view of the Saracen Castle and the south face of the cliff; (**c**) panoramic view of the cliff from the main square of Taormina; (**d**) block fallen along PPS in 2015; (**e**) block fallen along PPS in 2013; (**f**) unstable, loosened blocks occurring along the cliff.

3. Geomechanical and Kinematic Analysis of Rock Masses

From a lithological point of view, the cliff is made of greyish-white limestones and dolostones. There is not a definite limit between these two rock types, as limestones are partly or completely dolomitized. In particular, dolostones are characterized by a higher degree of fracturing due to their brittle behavior under stress. Laboratory tests, carried out on intact rock specimens at the Laboratory of Applied Geology of the Department of Biological, Geological, and Environmental Sciences of University of Catania, revealed that such rock type is characterized by a low total porosity ($\leq$10%) and average Uniaxial Compressive Strength ranging between 40 and 150 MPa. This relevant variability in the mechanical strength of the rock is linked to the presence of randomly oriented microcracks acting

as weakening elements within the rock structure [38–41]. Such outcome allows for the classification of the strength of tested specimens from "medium" to "high" according to [27].

Rock mass surveys, aimed at assessing the geomechanical condition of the cliff, were carried out at 8 measurement stations according to the recommendations proposed by the International Society for Rock Mechanics [27,28]. Such survey spots were located according to the accessibility of the area, which is affected by bad logistics due to steep sectors and hardly reachable outcrops. Dip-immersion, persistence, spacing, opening, in-filling, roughness, uniaxial compressive strength (UCS), and hydraulic conditions have been measured and evaluated along scan lines for each discontinuity. The orientation of discontinuities was statistically analyzed to group data into systems by plotting pole coordinates into a lower hemispheric projection net. A statistical contouring was carried out to evaluate mean and maximum pole concentrations, as well as to visualize the clustering of orientation [3]. Contours highlight the statistical concentration of poles calculated using the Fisher distribution method [42]. Such procedure allowed for the recognition of 4 to 6 discontinuity systems (Figure 4), although data are affected by a degree of scattering, due to the intense tectonic history experienced by the outcrops. Discontinuities are characterized by variable spacing (from close to wide), tight to moderate aperture, and variable Joint Roughness Coefficient (Table 1). The most open discontinuities are sometimes filled with hard or soft material, indicating a certain rate of water circulation within the rock mass. This is a key element supporting instability features, since water circulation favors weathering and worsening of the mechanical attitude of rocks (e.g., [5,12,43,44]). Persistence of discontinuities is a hard parameter to evaluate, and it affects the slope modeling. The most persistent set is the bedding surface, evident along the cliff and showing a sub-horizontal asset. This set is cut by orthogonal systems with unfavorable geometries from the stability point of view. Such setting is in accordance with the geomechanical condition of neighboring outcrops, recently studied for stability purposes also through innovative remote survey methodologies [44–47]. All of the geomechanical parameters surveyed in the field were employed to classify rock masses according to the Rock Mass Rating classification system [48]. This combines the most significant geostructural and geomechanical parameters by scoring them to calculate a comprehensive index of rock mass quality (RMR), usually employed for design and construction of excavations, foundations, and consolidation works. According to this procedure, studied rock masses can be classified as "fair rock" (RMR between 41 and 60) and are characterized by a cohesion ranging from 240 to 295 kPa and internal friction angle from 29 to 34° (Table 1).

Once the discontinuity systems and their geometrical relationship with the slope face were identified, kinematic analysis was carried out to give an indication of the stability condition of the cliff. To this purpose, the main kinematic patterns were taken into account to assess their possible occurrence. Such procedure highlighted that all the surveyed rock masses are affected by unfavorable kinematic orientation of discontinuities, resulting in unstable features. The most common unstable pattern is the planar sliding, which is revealed at all the surveyed outcrops when a discontinuity plane dips at a flatter angle than the face, with a dip direction differing from the dip direction of the face by no more than about 20°. This gains specific relevance considering that the slope face is characterized by abrupt changes in strike and, therefore, almost all the systems could be involved in this type of failure when they are in unfavorable condition. A similar consideration can be carried out for toppling, which is recognizable at the surfaces dipping into the slope face. On the other hand, the intersection between two or three discontinuity planes gives rise to unstable wedge configurations at each surveyed rock mass; this failure pattern involves also several random planes, with critical intersections between the mean planes of grouped sets at stations 1-2-3-6-7, indicating that instability mechanisms are not related only to the main discontinuity families.

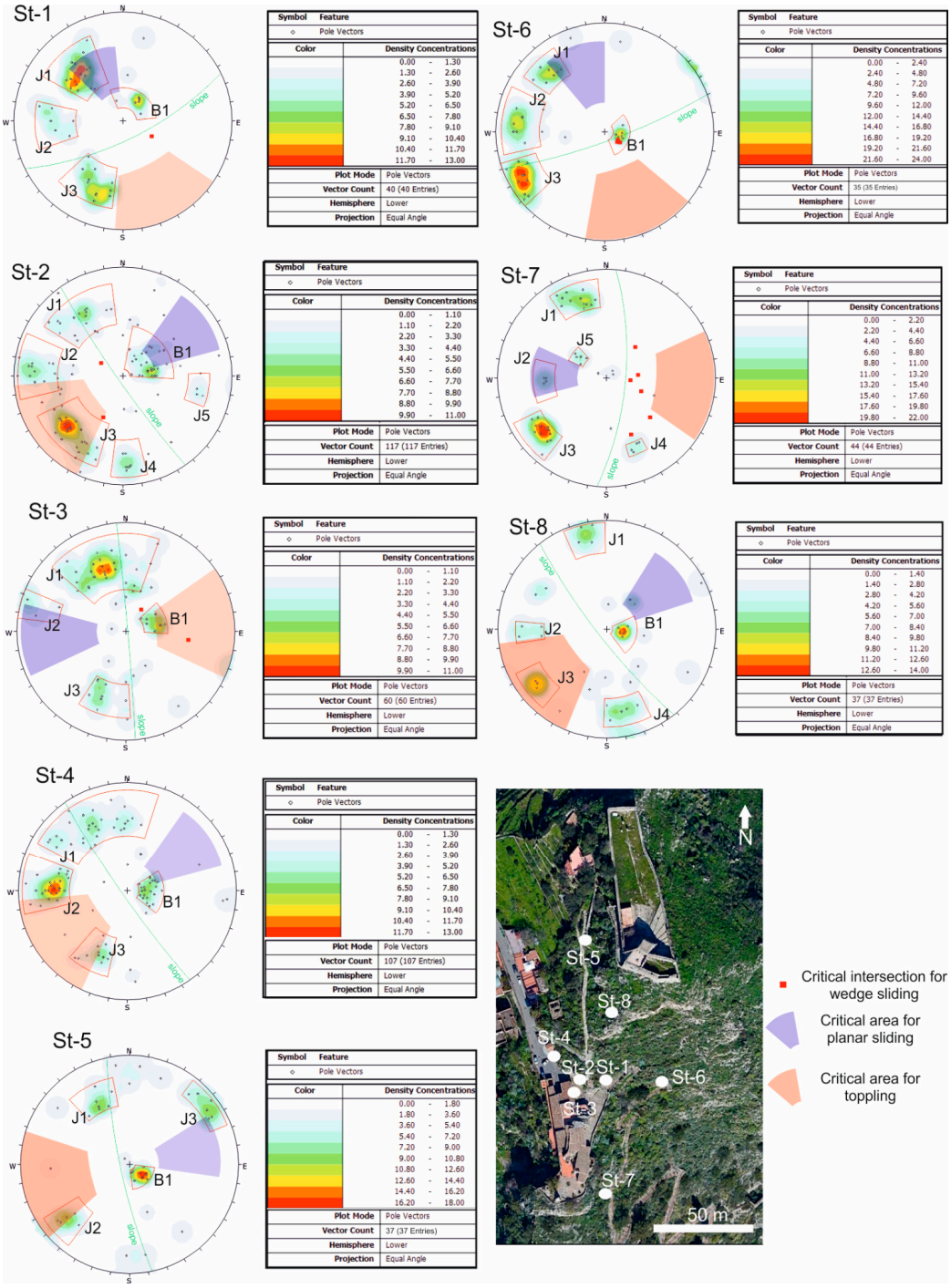

Figure 4. Stereonets of surveyed rock masses showing the contour plots of the main discontinuity sets along with the critical areas for the main unstable kinematic patterns.

Table 1. Main geomechanical parameters surveyed at each measurement station.

	Set	Spacing (mm)	Persistance (m)	Aperture (mm)	JRC	Infilling	Weathering	RMR Class
St-1 (slope 154/70)	J1 (138/60)	Close (60–200)	High (10–20)	Moderate (2.5–10)	4–6	none	Moderate	52 III Fair rock
	J2 (090/63)	Close (60–200)	Medium (3–10)	Moderate (2.5–10)	2–4	soft	Moderate	
	J3 (023/64)	Moderate (200–600)	Medium (3–10)	Moderate (2.5–10)	4–6	soft	Moderate	
	B1 (213/23)	Close (60–200)	Very high (>20)	Partly open (0.25–0.5)	2–4	none	Slight	
St-2 (slope 235/84)	J1 (143/66)	Close (60–200)	High (10–20)	Very tight (<0.1)	2–4	none	Moderate	56 III Fair rock
	J2 (093/75)	Close (60–200)	Medium (3–10)	Moderate (2.5–10)	2–4	none	Slight	
	J3 (043/70)	Close (60–200)	Medium (3–10)	Partly open (0.25–0.5)	6–8	none	Slight	
	J4 (357/78)	Close (60–200)	Low (1–3)	Very tight (<0.1)	10–12	none	Slight	
	J5 (279/71)	Moderate (200–600)	Medium (3–10)	Partly open (0.25–0.5)	6–8	soft	Slight	
	B1 (243/28)	Close (60–200)	Very high (>20)	Very tight (<0.1)	14–16	none	Slight	
St-3 (slope 080/88)	J1 (165/62)	Close (60–200)	High (10–20)	Very tight (<0.1)	4–8	none	Moderate	53 III Fair rock
	J2 (107/81)	Veryclose (20–60)	Medium (3–10)	Partly open (0.25–0.5)	6–8	none	Slight	
	J3 (021/63)	Close (60–200)	Medium (3–10)	Very tight (<0.1)	6–8	none	Slight	
	B1 (253/30)	Close (60–200)	Very high (>20)	Very tight (<0.1)	4–8	none	Slight	
St-4 (slope 235/84)	J1 (159/67)	Close (60–200)	High (10–20)	Very tight (<0.1)	2–8	none	Moderate	53 III Fair rock
	J2 (093/69)	Veryclose (20–60)	Medium (3–10)	Moderate (2.5–10)	2–4	soft	Slight	
	J3 (026/65)	Close (60–200)	Medium (3–10)	Very tight (<0.1)	4–8	none	Slight	
	B1 (269/22)	Close (60–200)	Very high (>20)	Partly open (0.25–0.5)	2–4	none	Slight	
St-5 (slope 258/80)	J1 (154/64)	Close (60–200)	High (10–20)	Moderate (2.5–10)	8–12	soft	Slight	56 III Fair rock
	J2 (048/75)	Close (60–200)	Medium (3–10)	Very tight (<0.1)	4–8	none	Slight	
	J3 (232/84)	Moderate (200–600)	Medium (3–10)	Partly open (0.25–0.5)	2–4	none	Slight	
	B1 (314/16)	Moderate (200–600)	Very high (>20)	Very tight (<0.1)	4–8	none	Slight	
St-6 (slope 160/80)	J1 (140/72)	Close (60–200)	High (10–20)	Partly open (0.25–0.5)	2–8	hard	Slight	52 III Fair rock
	J2 (094/70)	Close (60–200)	Medium (3–10)	Partly open (0.25–0.5)	8–12	soft	Moderate	
	J3 (060/82)	Close (60–200)	Medium (3–10)	Partly open (0.25–0.5)	2–4	none	Slight	
	B1 (253/30)	Close (60–200)	Very high (>20)	Very tight (<0.1)	4–8	none	Slight	
St-7 (slope 095/70)	J1 (159/75)	Close (60–200)	High (10–20)	Moderate (2.5–10)	6–12	soft	Moderate	53 III Fair rock
	J2 (088/59)	Close (60–200)	Medium (3–10)	Very tight (<0.1)	4–8	none	Moderate	
	J3 (050/75)	Close (60–200)	Medium (3–10)	Moderate (2.5–10)	8–12	none	Slight	
	J4 (337/69)	Close (60–200)	Low (1–3)	Partly open (0.25–0.5)	8–12	soft	Slight	
	J5 (127/34)	Close (60–200)	Low (1–3)	Partly open (0.25–0.5)	2–4	none	Slight	
St-8 (slope 232/80)	J1 (168/83)	Moderate (200–600)	High (10–20)	Moderate (2.5–10)	4–6	soft	Moderate	47 III Fair rock
	J2 (088/69)	Close (60–200)	Medium (3–10)	Moderate (2.5–10)	8–10	soft	Moderate	
	J3 (052/78)	Moderate (200–600)	Medium (3–10)	Moderate (2.5–10)	14–16	soft	Moderate	
	J4 (350/74)	Moderate (200–600)	Medium (3–10)	Moderate (2.5–10)	2–4	soft	Moderate	
	B1 (278/17)	Close (60–200)	Very high (>20)	Very tight (<0.1)	2–4	none	Moderate	

4. Terrestrial Laser Scanner Survey

Terrestrial Laser Scanning (TLS) is a ground-based remote sensing technique used in different geological fields to overcome the limits of traditional surveying methods. Joined with the topographic approach, the TLS technique can produce point cloud data to obtain high-resolution 3D surface models. In recent years, TLS has been exploited for different engineering geological tasks, including rockfall stability analysis [2,49], geomorphological and geostructural analyses of coastal cliffs [50–52], environmental monitoring of deformations, displacement and landslides [53], and discontinuity analysis of rock slopes (e.g., [54–56]). The great advantage provided by TLS technique is the possibility to obtain a 3D output model of the scanned element with the accuracy of the best topographic instruments. Moreover, if used in different times, the TLS outputs can be compared to estimate relative displacements (e.g., for monitoring slow-moving landslides).

In this paper, TLS was coupled with the topographic approach to obtain an accurate 3D model of the upper sector of the southern Taormina cliff. A laser scanner Leica P20, working in a range of 120 m and a rate of 1,000,000 points/s, was employed. Leica P20 also provides an integrated 5-megapixel camera to produce photos during the scanning process.

Three survey points were chosen to carry out TLS measurements at the southern sector of the cliff, which is characterized by a sub-vertical slope at its higher portion. This approach allowed for the achievement of a well-defined point cloud of the scanned cliff, with an accuracy that respects the target data, namely 6 mm for a measure carried out at a distance of 100 m. This value has been extensively tested in different works performed using the same laser scanner [57] (Figure 5). Resulting point clouds were processed using the software Cyclone [58] by filtering data from noise and negligible parts, thus obtaining a georeferenced Digital Terrain Model (DTM). In particular, the point clouds were georeferenced using three vertices of known coordinates in UTM-WGS84 and the final points cloud, with 27,580,698 points produced with a point density of 20,000 per square meter. (Figure 5).

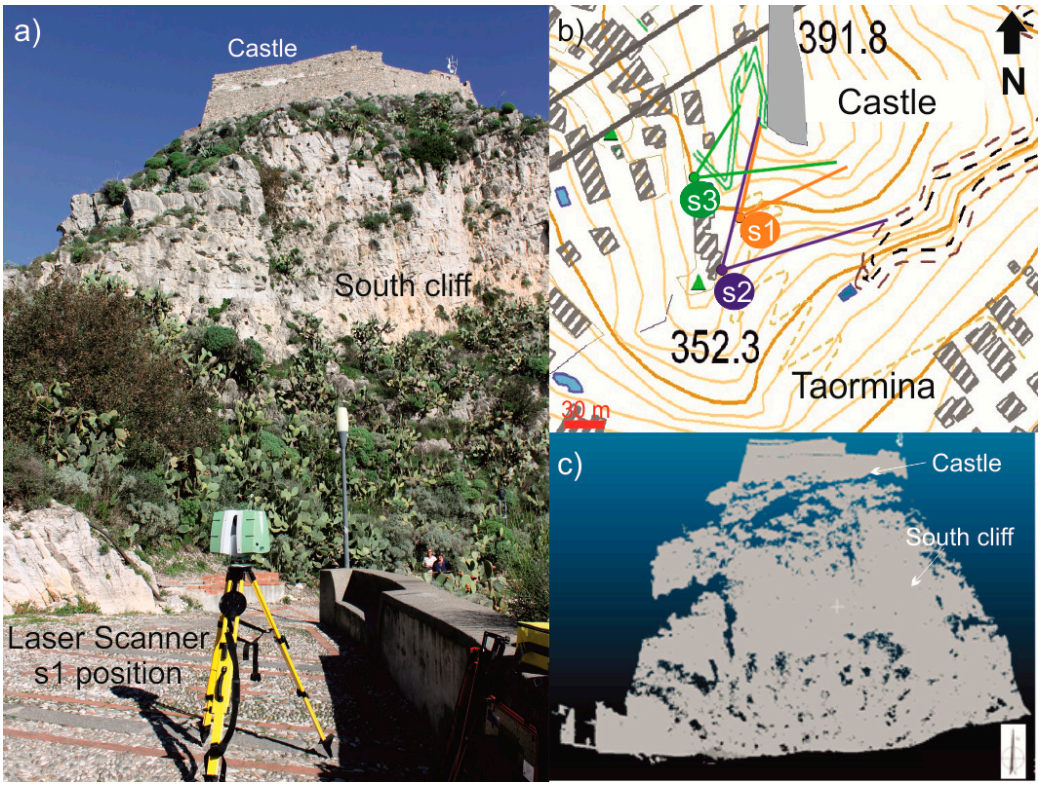

Figure 5. (**a**) Field setting during the TLS survey at s1 position (see inset b); (**b**) TLS survey spots reported on a topographic map; (**c**) point cloud of the south cliff.

5. Rockfall Simulations

Rockfall potential trajectories were simulated on 3D and 2D models with the aim of evaluating their spatial distribution, and of assessing the kinetic energy of falling boulders. Such analysis, which was preparatory to the hazard assessment discussed in the following section, was carried out by considering boulders with an average volume of 0.15 m^3, which were similar in size to those already fallen in the area in the recent years. Due to a lack of precise information on the rockfall history of the cliff, the most reliable datum on the block volume is represented by the latest documented events described in previous sections (Figure 3).

The 3D model of the cliff was generated by overlapping the DTM obtained by TLS surveys with its corresponding portion in a DTM with a 2 m regular grid of the whole study area (having the same reference system), provided for scientific purposes by Assessorato Territorio e Ambiente of Regione Siciliana. Such procedure was aimed at achieving a better morphological detail of the vertical southern cliff portion.

Falling blocks were simulated as spheres rotating around their center of gravity by Georock 3D [59], detaching them from a pre-established "launch" site. Their motion is described by impacts on an elevation-attributed plane represented by a grid of tridimensional nodes forming a triangular mesh, which is the entire area between the launch and the stopping points of the blocks [8].

Coefficients of restitutions were retrieved by literature, according to back analysis performed in similar and neighboring contests [8,19,20] (Table 2). Simulations took into account the potential detachment points, mainly identified on site at the highest portions of the cliff, and the presence of widespread blocks previously fallen and stopped along the slope, which are likely to be mobilized giving rise to new rockfall events. The presence of local protection barriers or remedial works was not considered herein, erring on the side of caution, due to their limited catching area and to their unknown conditions of maintenance. In fact, cases of falling boulders bypassing existing rockfall barriers are not rare in the study area [8].

Table 2. Coefficients of restitutions considered for rockfall trajectory simulations (after [8]). R_n: normal component; R_t: tangential component.

Material	R_t	R_n
Bare rock	0.80	0.50
Rock and vegetation	0.74	0.24
Rock debris	0.65	0.15
Asphalt	0.90	0.40

The distribution of ten thousand simulated trajectories (Figure 6) shows that almost all the simulated patterns reach the buildings at the foot of cliff and affect PPS, thus representing a relevant threat for safety of inhabitants and tourists. The sectors showing the main reception of falling blocks are located northeast and southeast, where the morphology of the cliff allows the concentration of trajectories. According to the achieved distribution of the 3D model, then represented by a satellite image (Figure 6), 2D simulations were carried out on adjacent sections to analyze the kinetic energy reached during the block route (Figure 6). In this case, rockfall trajectories were simulated along 2D slope sections according to the Lumped Mass method, which is based on a particle analysis [60]; each boulder is considered as a particle with a constant mass during the simulation. This latter parameter is used only to calculate the rock kinetic energy, whose value is provided as the highest kinetic energy that any rock attained while passing each horizontal location along the section. By adopting the Lumped Mass approach, the kinetic energy of a falling boulder can be calculated by:

$$E = \frac{1}{2} m\, v^2 \quad (1)$$

in which E is the kinetic energy, m is the mass of the rock block, and v is the falling velocity [61].

Estimated energy ranges from 10 to 320 kJ. Minimum values are found at the top of the cliff, which contains the detachment sectors, where the block movement is mainly represented by rolling motions along the slope face. On the other hand, the highest kinetic energy values are found in the lower sector of the southeastern cliff, where, due to an abrupt change in the slope gradient (scarp), boulders gain energy through free-fall and rebound motions (Figure 7). Vegetation plays a slowing role on the movement, although this positive action is strictly connected to the presence of shrubs and trees. In case of fires, which are common events that occur annually in this sector of Sicily, currently vegetated sectors would be bared, and their braking action would be no longer effective, thus representing a bad consequence to be taken into account for potential further and more detailed analyses due to the possible increase of kinetic energy.

An interesting element to point out is the presence of a medium-high energy corridor, affecting the southern sector of the cliff from its top. Such great values are enhanced by the scarp at the base of the Saracen Castle (Figure 7), which breaks the rolling movement of boulders favoring their free fall along the slope (involving also PPS) until the downstream houses and road. This must be regarded as a key sector, due to the presence of PPS traveled by numerous tourists all year long.

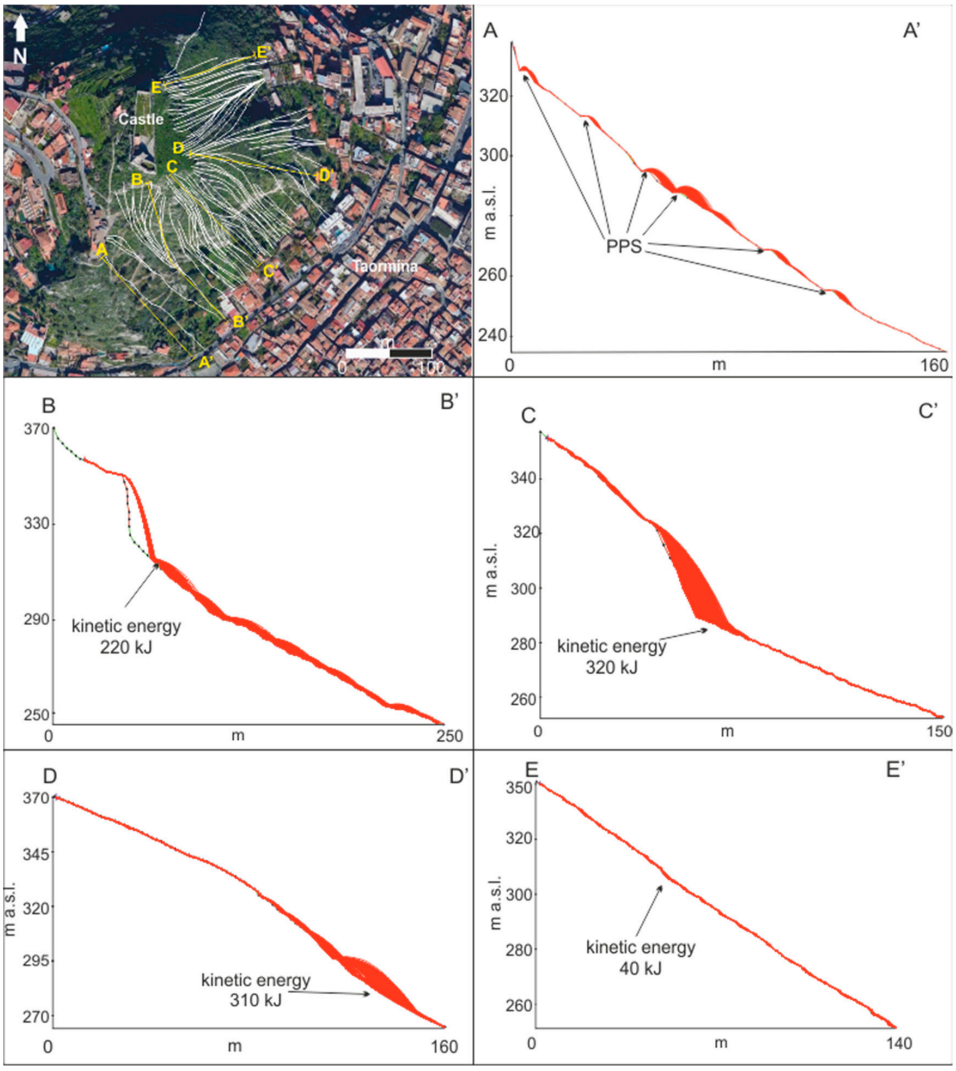

Figure 6. Simulated rockfall trajectories: the map shows the spatial distribution of trajectories simulated on a 3D model (white paths), along with the traces (yellow lines) of the reported representative 2D sections.

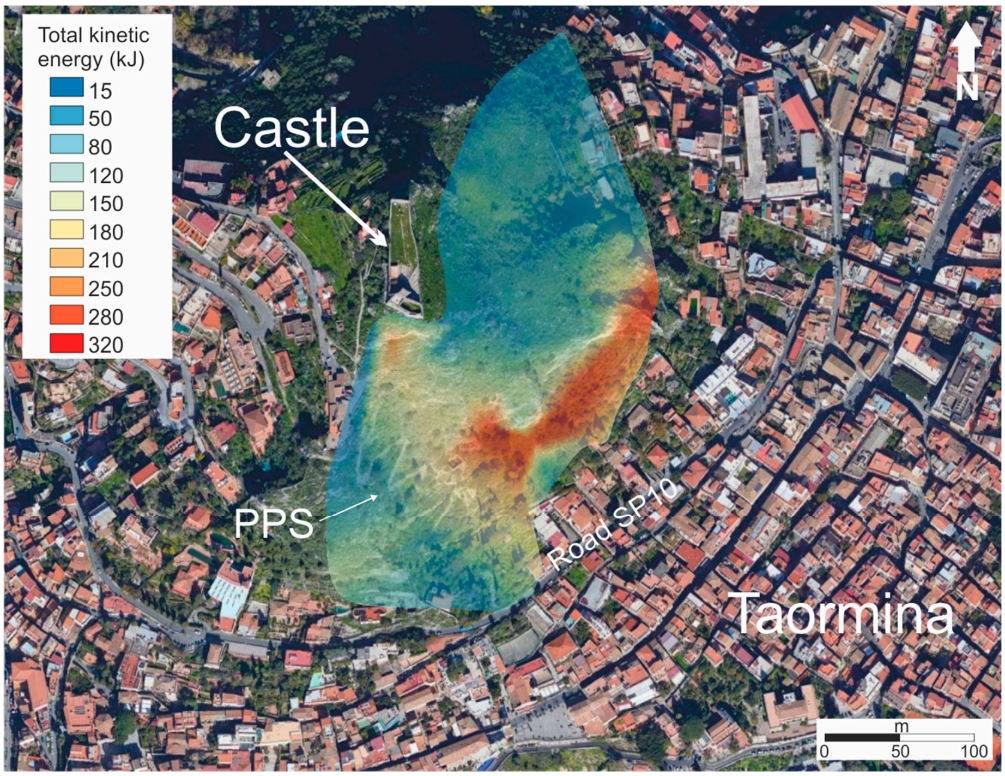

Figure 7. Contour map showing the spatial distribution of kinetic energy values resulting from trajectory simulations.

6. Evolving Rockfall Hazard Assessment

Several authors proposed risk assessment procedures, applied to peculiar case studies worldwide (e.g., [8,12,16–19]). The utility of this kind of study is a zonation of the hazard to set up a strategy management of the faced problems, with particular reference to possible activation of emergency procedures, such as warnings and evacuations.

The Evolving Rockfall Hazard Assessment (ERHA) is a qualitative methodology designed for the Australian open-pit coal-mining environment and proposed in Switzerland for landslide risk management purposes. It is aimed at the identification of the most hazardous areas along a slope [25] based on the employment of a 3 × 3 matrix showing the probability of occurrence and the intensity of the studied phenomenon along the horizontal and vertical axes, respectively (Figure 8). Cells of the matrix are labelled low, medium, and high to indicate the level of hazard, growing proportionally with the probability of occurrence and the intensity of the event [24,25]. As a qualitative method, this is the first active stage of a risk assessment procedure and can be taken as reference for further quantitative approaches focused on the targets of potential rockfalls. For simplicity in reading, the method is described in the following way with reference to the case study presented herein.

ERHA matrix is built considering (1) the state of activity of the slope and (2) the rockfall impact (i.e., intensity) (Figure 8).

(1) The state of activity is related to the geomechanical condition of studied slopes. This is described by a score resulting from the rating of the geological structure of the rock (degree of rock mass fracturing), the potentially unstable patterns (kinematic setting), and the slope performance (signs of past detachments) (Tables 3 and 4, after [25]). The degree of fracturing of rock mass is mainly related to the number, arrangement, and persistence of discontinuity sets. In particular, ERHA method takes into account three rock mass structures, i.e., intact, blocky, and very blocky, based on the number of discontinuity systems (few sets for intact, three for blocky, four or more

sets for very blocky categories) [24]. In this case, all these data were retrieved from the rock mass surveys, which allowed the recognition of 4 to 6 main discontinuity systems (very blocky structure) (Table 3).

Weathering is present along both the slope face and the open discontinuity planes, while kinematic analysis highlighted that planar sliding and toppling failures can be regarded as unstable patterns. Finally, signs of past detachments are widespread along the cliff, as previously addressed. All these elements allowed scoring 9 as final value of state of activity, which would have turned into 11 in case of differential weathering. In any case, it corresponds to a "high" state of activity class (Table 4). It has to be underlined that, even with a lower "state of activity" score (for example between 4 and 7 in Table 4), slopes with signs of activity are anyhow considered with a "high" state of activity according to Table 4; therefore, the main variable in this analysis is the rockfall intensity following described.

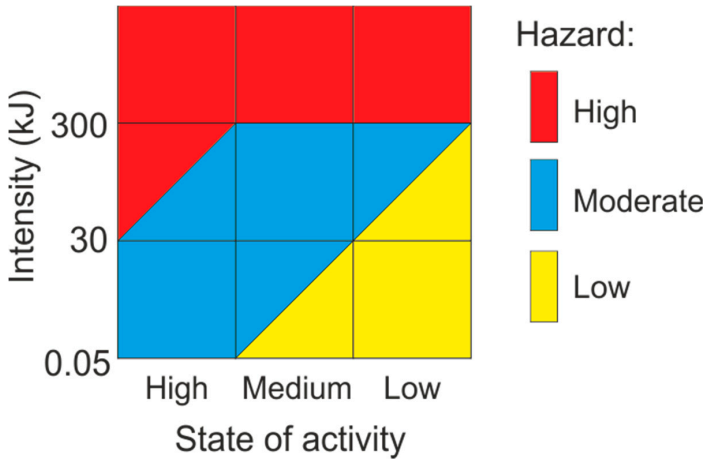

Figure 8. Hazard matrix (modified after [24,25]).

Table 3. Parameters, ratings, and weights for evaluating the preliminary state of activity score (after [25]).

Parameter	Description	Rating	Weight	Score
Fracturing Degree	Massive rock mass Blocky or very blocky rock mass	0 1	3	3
Undercutting	Homogeneous weathering Differential weathering	0 1	2	0
Block sliding	Unlikely Likely	0 1	2	2
Block toppling	Unlikely Likely	0 1	1	1
Slope performance	Good Bad (signs of past detachments)	0 1	3	3
			Σ	**9**

Table 4. Stave of activity classes (after [25]).

Preliminary Score	Preliminary Class	Without Signs of Activity	With Signs of Activity
0–3	Low	Low	Medium
4–7	Medium	Medium	High
8–11	High	High	High

(2) Rockfall intensity is related to the impact energy in the exposed zone, which can be expressed by the total kinetic energy estimated at a defined impact point.

Due to the necessity of defining an energy boundary between the intensity classes, 300 kJ was taken as a limit between high and medium classes, since it corresponds to the energy that can be resisted by a properly built reinforced concrete wall. Similarly, 30 kJ, representing the maximum energy that oak wood stiff barriers (railway sleepers) can resist [24], was considered as the energy limit between medium and low classes in the matrix (Figure 8).

For this case study, and according to Figure 7, considering that the state of activity is "high" along the whole cliff, the final hazard is function of the kinetic energy of rockfalls, estimated herein between 10 and 320 kJ by trajectory simulations.

As a result, hazard varies between Moderate and High values as summarized in Figure 9, in which a contour map highlighting the variation of hazard based on achieved results is reported. The highest hazard affects the southeastern cliff, with particular reference to the downstream portions, which constitute the inhabited sector. This is a key result, because it proves the existence of a level of risk, which cannot be underestimated. High hazard is found also at the steeper eastern sectors of the cliff, while PPS is in a moderate-to-high hazard corridor, in which kinetic energy of boulders is variable with respect to the rebound points, presence of vegetation, and scarps. Nevertheless, this is another sector at risk due to the daily transit of people reaching the upstream castle.

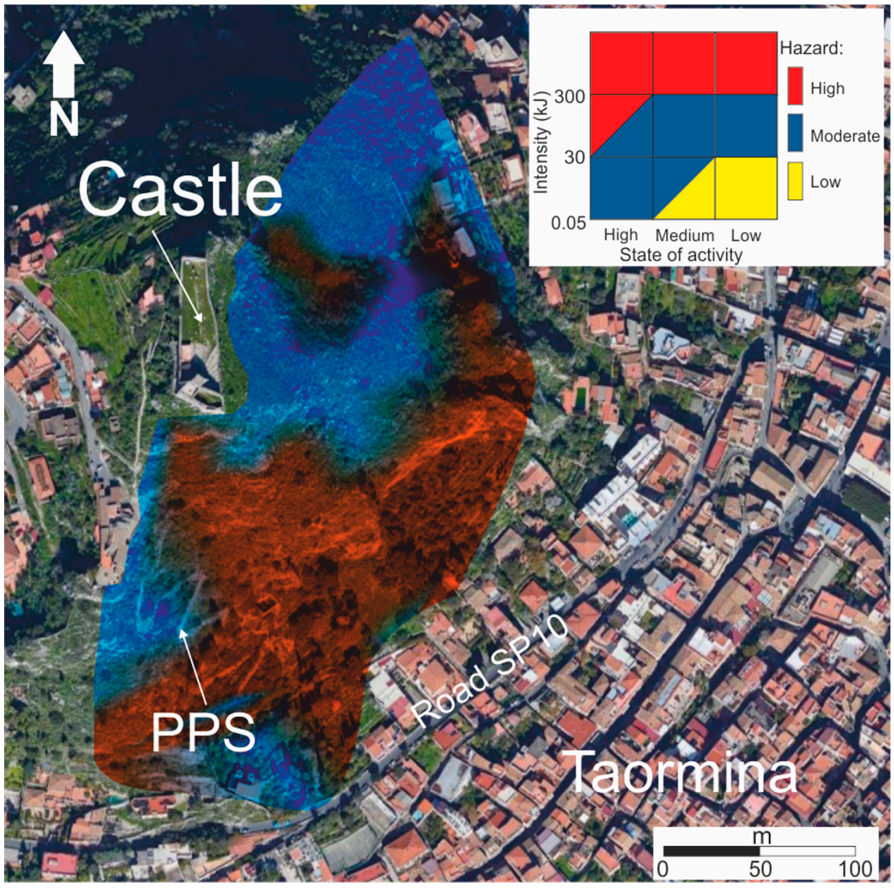

Figure 9. Hazard map of the Taormina rock cliff.

7. Discussion and Conclusions

A qualitative approach for rockfall hazard zonation is applied herein to a peculiar part of northeastern Sicily, where the carbonate cliff of Taormina dominates the Ionian coastline. The Evolving Rockfall Hazard Assessment is inspired by the widely acknowledged Swiss guidelines for rockfall hazard, which define different hazard levels based on the probability of occurrence and the intensity of rockfalls. The first one is redefined by EHRA as the state of activity of the slope, assessable by means

of a rating-based procedure, while the intensity of rockfalls is estimated through rockfall trajectory simulations. This approach is a valid scientific tool for preliminary hazard zonation and allows for the highlighting of the main criticalities of a specific area. In this paper, the carbonate cliff on which the Saracen Castle of Taormina is perched is the focus of EHRA application. It has been affected by serious rockfalls over the years, although most of the events were never studied or documented, which mainly threatened the downstream inhabited center and a pedestrian tourist path (PPS) connecting the city to the castle.

The study area has a strategic relevance due to its location and history; in fact, the Saracen Castle is part of the cultural heritage as witness of the defensive architecture of XII and XIII centuries. The complex geological history of the site, part of the orogenic context of Peloritani Mountains, is the main factor responsible of the high degree of fracturing of rock masses, studied herein by rock mass surveys, and carried out at eight measurement stations. Due to the bad logistics of the area, stations were located according to the availability of suitable rock walls to the survey and to the accessibility of the cliff. Discontinuities were grouped into 4 to 6 systems, most of which affect dolostone outcrops, in which the degree of fracturing is enhanced by the brittle behavior of such rock types and the rock volume is centimetric. At limestones, the wider spacing defines greater volumes of rock, which represents the most worrying feature from the risk management point of view. In fact, boulders that recently detached and fell along PPS had volumes of about 0.15 m^3. Kinematic analysis highlighted the predisposition of the rock mass to fail through planar and wedge sliding and toppling mechanisms. This kinematic setting, along with the geomechanical features surveyed in the field, provided reliable preliminary knowledge of the stability condition of the cliff and can be considered basic information for the assessment of the state of the activity of the slopes according to the ERHA method. In this preliminary stage, the cliff can be assumed as characterized by a "high" state of activity, mainly due to the unfavorable kinematic patterns, the intense degree of fracturing ("very blocky structure" of the rock mass), and the widespread signs of rockfall activity. On the other hand, rockfall intensity was estimated by simulating the potential trajectory of falling boulders, on 2D and 3D models, to assess their total kinetic energy. From the combination of the rock mass "state of activity" and rockfall intensity, the hazard level along the cliff ranges from Moderate to High. It is mainly a function of the intensity of rockfalls, which is higher in the foot of scarps and in steeper sectors, in which blocks move downwards through rebounds. This is an index of relevant risk, as the most hazardous area is at the foot of the cliff, where the inhabited center of Taormina and the road SP10 are among the main elements at risk. A similar consideration is for PPS, which lays within a corridor of moderate-to-high hazard that cannot be underestimated due to the strong touristic importance of this trail. Besides the relevance of this study for local risk management purposes, achieved results proved the utility of qualitative procedures for a preliminary zonation of the hazard arising from the occurrence of rockfalls, especially in cultural heritage sites, where often logistics and local restrictions make the field surveys uneasy. Moreover, EHRA results presented on thematic maps can be employed in the perspective of designing suitable mitigation works, to prevent the occurrence of rockfalls and/or reduce related consequences. Such an aspect is crucial for further in-depth studies dealing with the assessment of the acceptability of resulting risk, from the legal and administrative points of view, which aim to achieve acceptable levels of risk.

Acknowledgments: The research was financially supported by "Piano Triennale della Ricerca (2017–2020)" (University of Catania, Department of Biological, Geological and Environmental Sciences), scientific responsible Giovanna Pappalardo. Laboratory tests were carried out at the Laboratory of Applied Geology of the same department. Terrestrial Laser Scanner is property of University of Catania, Department of Civil Engineering and Architecture, Laboratory of Geomatics scientific responsible Giuseppe Mussumeci. Authors would like to thank Claudio Sanfilippo for his friendly help during the first of the two campaigns of rock mass survey.

Author Contributions: Simone Mineo and Giovanna Pappalardo organized and coordinated the activities of rock mass surveys, geomechanical characterization of slopes, rockfall trajectory simulations, and hazard assessment. They wrote the article and coordinated the working group. Giuseppe Mussumeci and Michele Mangiameli carried out the TLS surveys and elaborated the related data. They also wrote the TLS section. Santo Campolo provided the historical characterization of the Saracen Castle.

Conflicts of Interest: The authors declare no conflict of interest.

References

1. Canuti, P.; Casagli, N.; Catani, F.; Fanti, R. Hydrogeological hazard and risk in archaeological sites: Some case studies in Italy. *J. Cult. Herit.* **2000**, *1*, 117–125. [CrossRef]
2. Fanti, R.; Gigli, G.; Lombardi, L.; Tapete, D.; Canuti, P. Terrestrial laser scanning for rockfall stability analysis in the cultural heritage site of Pitigliano (Italy). *Landslides* **2012**, *10*, 409–420. [CrossRef]
3. Pappalardo, G.; Imposa, S.; Mineo, S.; Grassi, S. Evaluation of the stability of a rock cliff by means of geophysical and geomechanical surveys in a cultural heritage site (south-eastern Sicily). *Ital. J. Geosci.* **2016**, *135*, 308–323. [CrossRef]
4. Chau, K.T.; Wong, R.H.C.; Liu, J.; Lee, C.F. Rockfall Hazard Analysis for Hong Kong Based on Rockfall Inventory. *Rock Mech. Rock Eng.* **2003**, *36*, 383–408. [CrossRef]
5. Dorren, L.K.A.; Seijmonsbergen, A.C. Comparison of three GIS-based models for predicting rockfall runout zones at a regional scale. *Geomorphology* **2003**, *56*, 49–64. [CrossRef]
6. Schneuwly, D.M.; Stoffel, M. Spatial analysis of rockfall activity, bounce heights and geomorphic changes over the last 50 years—A case study using dendrogeomorphology. *Geomorphology* **2008**, *102*, 522–531. [CrossRef]
7. Corominas, J.; Van Westen, C.; Frattini, P.; Cascini, L.; Malet, J.P.; Fotopoulou, S.; Catani, F.; Van Den Eeckhaut, M.; Mavrouli, O.; Agliardi, F.; et al. Recommendations for the quantitative analysis of landslide risk. *Bull. Eng. Geol. Environ.* **2014**, *73*, 209–263. [CrossRef]
8. Mineo, S.; Pappalardo, G.; D'Urso, A.; Calcaterra, D. Event tree analysis for rockfall risk assessment along a strategic mountainous transportation route. *Environ. Earth Sci.* **2017**, *76*, 620. [CrossRef]
9. Ball, D.; Watt, J. Risk management and cultural presentation. In Proceedings of the ARIADNE Workshop 4, Vulnerability of Cultural Heritage to Hazards and Prevention Measures, Prague, Czech Republic, 18–24 August 2001.
10. United Nations Educational, Scientific and Cultural Organization. *UNESCO Risk Management Training Handbook 2010*; BSP-2010/WS7; UNESCO: Paris, France, 2010.
11. Evans, S.G.; Hungr, O. The assessment of rockfall hazard at the base of talus slopes. *Can. Geotech. J.* **1993**, *30*, 620–636. [CrossRef]
12. Crosta, G.B.; Agliardi, F. A methodology for physically based rockfall hazard assessment. *Nat. Hazards Earth Syst. Sci.* **2003**, *3*, 407–422. [CrossRef]
13. Peila, D.; Guardini, C. Use of the event tree to assess the risk reduction obtained from rockfall protection devices. *Nat. Hazards Earth Syst. Sci.* **2008**, *8*, 1441–1450. [CrossRef]
14. Guzzetti, F.; Reichenbach, P. Rockfalls and their hazard. In *Tree Rings and Natural Hazards*; Stoffel, M., Bollschweiler, M., Butler, D.R., Luckman, B.H., Eds.; Springer: Berlin, Germany, 2010; pp. 129–137.
15. Saroglou, H.; Marinos, V.; Marinos, P.; Tsiambaos, G. Rockfall hazard and risk assessment: An example from a high promontory at the historical site of Monemvasia, Greece. *Nat. Hazards Earth Syst. Sci.* **2012**, *12*, 1823–1836. [CrossRef]
16. Ansari, M.K.; Ahmad, M.; Singh, T.N. Rockfall Risk Assessment along Mumbai-Pune Expressway, Maharashtra, India. *Int. J. Sci. Res.* **2014**, *3*, 424–426.
17. Pantelidis, L.; Kokkalis, A. Designing passive rockfall measures based on computer simulation and field experience to enhance highway safety. *Int. J. Rock Mech. Min. Sci.* **2011**, *48*, 1369–1375. [CrossRef]
18. Budetta, P.; Nappi, M. Comparison between qualitative and quantitative rockfall risk methods for a hazardous road stretch. Advances in Environmental and Agricultural Science. 2015, pp. 13–17. Available online: http://www.wseas.us/e-library/conferences/2015/Dubai/ABIC/ABIC-01.pdf (accessed on 1 Feburary 2018).
19. Pappalardo, G.; Mineo, S.; Rapisarda, F. Rockfall hazard assessment along a road on the Peloritani Mountains (northeastern Sicily, Italy). *Nat. Hazards Earth Syst. Sci.* **2014**, *14*, 2735–2748. [CrossRef]
20. Pappalardo, G.; Mineo, S. Rockfall Hazard and Risk Assessment: The Promontory of the Pre-Hellenic Village Castelmola Case, North-Eastern Sicily (Italy). In *Engineering Geology for Society and Territory*; Lollino, G., Manconi, A., Clague, J., Shan, W., Chiarle, M., Eds.; Springer International Publishing: Cham, Switzerland, 2015; Volume 2, pp. 1989–1993. [CrossRef]

21. Macciotta, R.; Martin, C.D.; Morgenstern, N.R.; Cruden, D.M. Quantitative risk assessment of slope hazards along a section of railway in the Canadian Cordillera—A methodology considering the uncertainty in the results. *Landslides* **2016**, *13*, 115–127. [CrossRef]
22. Pierson, L.A.; Davis, S.A.; Van Vickle, R. *Rockfall Hazard Rating System—Implementation Manual, Federal Highway Administration (FHWA)*; Report FHWAOR-EG-90-01, FHWA; US Department of Transportation: Washington, DC, USA, 1990.
23. Mignelli, C.; Lo Russo, S.; Peila, D. Rockfall risk Management assessment: The RO.MA. approach. *Nat. Hazards* **2012**, *62*, 1109–1123. [CrossRef]
24. Lateltin, O.; Haemmig, C.; Raetzo, H.; Bonnard, C. Landslide risk management in Switzerland. *Landslides* **2005**, *2*, 313–320. [CrossRef]
25. Ferrari, F.; Giacomini, A.; Thoeni, K.; Lambert, C. Qualitative evolving rockfall hazard assessment for highwalls. *Int. J. Rock Mech. Min. Sci.* **2017**, *98*, 88–101. [CrossRef]
26. Amari, M. *Biblioteca Arabo-Sicula*; Loescher: Torino/Roma, Italy, 1880; Volume 2.
27. International Society for Rock Mechanics (ISRM). Suggested methods for the quantitative description of discontinuities in rock masses. *Int. J. Rock Mech. Min. Sci.* **1978**, *15*, 319–368.
28. International Society for Rock Mechanics (ISRM). The complete ISRM suggested methods for rock characterization, testing and monitoring: 1974–2006. In *Suggested Methods Prepared by the Commission on Testing Methods*; Ulusay, R., Hudson, J.A., Eds.; Compilation Arranged by the ISRM Turkish National Group; International Society for Rock Mechanics: Ankara, Turkey, 2007; p. 628.
29. Argeri, G. *Storia di San Piero Patti: Attraverso gli Avvenimenti più Importanti della Sicilia*; Scuola Grafica Salesiana: Palermo, Italy, 1984.
30. Atzori, P.; Cirrincione, R.; Kern, H.; Mazzoleni, P.; Pezzino, A.; Puglisi, G.; Punturo, R.; Trombetta, A. The abundance of elements and petrovolumetric models of the crust in northeastern Peloritani Mountains (Site 8). In *The Abundance of Elements and Petrovolumetric Models in Nine Type Areas from the Crystalline Basements of Italy, with Some Geophysical and Petrophysical Data*; Sassi, F.P., Zanettin, B., Eds.; Accademia Nazionale delle Scienze detta deiXL: Roma, Italy, 2003; Volume 32, pp. 309–358.
31. Lentini, F.; Carbone, S.; Guarnieri, P. Collisional and postcollisional tectonics of the Apenninic-Maghrebian orogen (southern Italy). In *Geological Society of America Special Paper 409*; Geological Society of America: Boulder, CO, USA, 2006; pp. 57–81.
32. Cirrincione, R.; Fazio, E.; Ortolano, G.; Pezzino, A.; Punturo, R. Fault-related rocks: Deciphering the structural-metamorphic evolution of an accretionary wedge in a collisional belt, NE Sicily. *Int. Geol. Rev.* **2012**, *54*, 940–956. [CrossRef]
33. Boschi, E.; Ferrari, G.; Gasperini, P.; Guidoboni, E.; Smriglio, G.; Valensise, G. *Catalogo dei Forti Terremoti in Italia dal 461 a.C. al 1980*; ING-SGA; Istituto Nazionale di Geofisica: Rome, Italy, 1995.
34. Catalano, S.; De Guidi, G.; Monaco, C.; Tortorici, G.; Tortorici, L. Long-term behaviour of the late Quaternary normal faults in the Straits of Messina area(Calabrian arc): Structural and morphological constraints. *Quat. Int.* **2003**, *101–102*, 81–91. [CrossRef]
35. Dumas, B.; Gueremy, P.; Raffy, J. Evidence for sea-level oscillations by the "characteristic thickness" of marine deposits from raised terraces of SouthernCalabria (Italy). *Quat. Sci. Rev.* **2005**, *244*, 2120–2136. [CrossRef]
36. Argnani, A.; Brancolini, G.; Bonazzi, C.; Rovere, M.; Accaino, F.; Zgur, F.; Lodolo, E. results of the Taormina 2006 seismic survey: Possible implications for active tectonics in the Messina Straits. *Tectonophysics* **2009**, *476*, 159–169. [CrossRef]
37. Borrelli, L.; Gullà, G. Tectonic constraints on a deep-seated rock slide in weathered crystalline rocks. *Geomorphology* **2017**, *290*, 288–316. [CrossRef]
38. Pappalardo, G. Correlation between P-Wave Velocity and Physical–Mechanical Properties of Intensely Jointed Dolostones, Peloritani Mounts, NE Sicily. *Rock Mech. Rock Eng.* **2015**, *48*, 1711–1721. [CrossRef]
39. Pappalardo, G.; Mineo, S. Microstructural controls on physical and mechanical properties of dolomite rocks. *Rend. Online Soc. Geol. Ital.* **2016**, *41*, 321–324. [CrossRef]
40. Pappalardo, G.; Mineo, S. Investigation on the mechanical attitude of basaltic rocks from Mount Etna through InfraRed Thermography and laboratory tests. *Constr. Build. Mater.* **2017**, *134*, 228–235. [CrossRef]
41. Pappalardo, G.; Punturo, R.; Mineo, S.; Contrafatto, L. The role of porosity on the engineering geological properties of 1669 lavas from Mount Etna. *Eng. Geol.* **2017**, *221*, 16–28. [CrossRef]
42. Fisher, R.A. Dispersion on a sphere. *Proc. R. Soc. Lond. Ser. A* **1953**, *217*, 295–305. [CrossRef]

43. Mineo, S.; Pappalardo, G.; Rapisarda, F.; Cubito, A.; Di Maria, G. Integrated geostructural, seismic and infrared thermography surveys for the study of an unstable rock slope in the Peloritani Chain (NE Sicily). *Eng. Geol.* **2015**, *195*, 225–235. [CrossRef]
44. Pappalardo, G.; Mineo, S.; Perriello Zampelli, S.; Cubito, A.; Calcaterra, D. InfraRed Thermography proposed for the estimation of the Cooling Rate Index in the remote survey of rock masses. *Int. J. Rock Mech. Min. Sci.* **2016**, *83*, 182–196. [CrossRef]
45. Mineo, S.; Calcaterra, D.; Perriello Zampelli, S.; Pappalardo, G. Application of Infrared Thermography for the survey of intensely jointed rock slopes. *Rend. Online Soc. Geol. Ital.* **2015**, *35*, 212–215. [CrossRef]
46. Pappalardo, G.; Mineo, S.; Calcaterra, D. Geomechanical Analysis of Unstable Rock Wedges by Means of Geostructural and Infrared Thermography Surveys. *Ital. J. Eng. Geol. Environ.* **2017**, 93–101. [CrossRef]
47. Pappalardo, G. First results of infrared thermography applied to the evaluation of hydraulic conductivity in rock masses. *Hydrogeol. J.* **2017**, 1–12. [CrossRef]
48. Bieniawski, Z.T. *Engineering Rock Mass Classification*; John Wiley & Son: New York, NY, USA, 1989; 251p.
49. Tavani, S.; Arbues, P.; Snidero, M.; Carrera, N.; Munoz, A. Open Plot Project: An open-source toolkit for 3-d structural data analysis. *Solid Earth* **2011**, *2*, 53–63. [CrossRef]
50. Lim, M.; Petley, D.N.; Rosser, N.U.; Allison, R.J.; Long, A.J.; Pybus, D. Combined digital photogrammetry and time-of-flight lase scanning for monitoring cliff evolution. *Photogramm. Rec.* **2005**, *20*, 109–129. [CrossRef]
51. Rosser, N.U.; Petley, D.N.; Lim, M.; Dunning, S.A.; Allison, R.J. Terrestrial laser scanning for monitoring the processo f hard rock coastal cliff erosion. *Q. J. Eng. Geol. Hydrogeol.* **2005**, *38*, 363–375. [CrossRef]
52. Matano, F.; Pignalosa, A.; Marino, E.; Esposito, G.; Caccavale, M.; Caputo, T.; Sacchi, M.; Somma, R.; Troise, C.; De Natale, G. Laser Scanning Application for Geostructural analysis of Tuffaceous Coastal Cliffs: The case of Punta Epitaffio, Pozzuoli Bay, Italy. *Eur. J. Remote Sens.* **2015**, *48*, 615–637. [CrossRef]
53. Gordon, S.; Lichti, D.; Stewart, M. Application of high-resolution, ground based laser scanner for deformation measurements. In Proceedings of the 10th International FIG Symposium on Deformation Measurements, Orange, CA, USA, 19–22 March 2001; pp. 23–32.
54. Slob, S.; Van Knapen, B.; Hack, R.; Turner, K.; Kemeny, J. Method for Automated Discontinuity Analysis of Rock Slopes with Three-Dimensional Laser Scanning. *J. Transp. Res. Board* **2005**, *1913*, 187–194. [CrossRef]
55. Abellán, A.; Oppikofer, T.; Jaboyedoff, M.; Rosser, N.J.; Lim, M.J.; Lato, M. Terrestrial laser scanning of rock slope instabilities. *Earth Surf. Process. Landf.* **2013**, *39*, 80–97. [CrossRef]
56. Matano, F.; Iuliano, S.; Somma, R.; Marino, E.; Del Vecchio, U.; Esposito, G.; Molisso, F.; Scepi, G.; Grimaldi, G.M.; Pignalosa, A.; et al. Geostructure of Corogliotuffcliff, Naples (Italy) derived from terrestrial laser scanner data. *J. Maps* **2016**, *12*, 407–421. [CrossRef]
57. Mangiameli, M.; Mussumeci, G.; Zito, S. Low cost digital photogrammetry: From the extraction of point clouds by SFM technique to 3D mathematical modeling. In Proceedings of the International conference of numerical analysis and applied mathematics, Rhodes, Greece, 19–25 September 2016; Volume 1863. [CrossRef]
58. Software "Cyclone". Available online: http://www.leica-geosystems.it/it/Leica-Cyclone_6515.htm (accessed on 5 February 2018).
59. Geostru. *Georock 3D User Manual*; Geostru: Cluj-Napoca, Romania, 2013.
60. Hoek, E. *Rockfall—A Program in Basic for the Analysis of Rockfalls from Slopes*; Department of Civil Engineering, University of Toronto: Toronto, ON, USA, 1987.
61. Macciotta, R.; Martin, C.D.; Cruden, D.M. Probabilistic estimation of rockfall height and kinetic energy based on a three-dimensional trajectory model and Monte Carlo simulation. *Landslides* **2015**, *12*, 757–772. [CrossRef]